STRAIN ANALYSIS OF MASSETER MUSCLE BY ULTRASOUND

A. BUSATO[1], G. BALCONI[2], V. VISMARA[1], L. BERTELÈ[3], G. TONTI[4] and G. PEDRIZZETTI[5]

[1]Medica Libra, Milano, Italy; [2]Department of Radiology, Hospital San Raffaele Turro, Milano, Italy; [3]Fondazione Apostolo, Merate, Italy; [4]Cardiology Division, "G. d'Annunzio" University, Chieti, Italy; [5]Department of Engineering and Architecture, University of Trieste, Italy

The masseter muscle represents an area of important functional interest. The present study aims to verify the feasibility of ultrasound imaging for quantifying the muscular deformation pattern in the masseter. Fifteen consecutive subjects were enrolled and underwent masseter ultrasound according to a repeatable protocol. Ultrasound was carried out during teeth clenching in natural conditions and after the insertion of a medical device that alters the distance between the dental arches, and was repeated on 3 different days. Results showed that masseter deformation is not uniform within the muscle. The same strain patterns were repeated in the different ultrasounds of the same patient and were modified after the introduction of a medical device. This was supported by quantitative comparisons in the deep portion of the muscle (standard deviation on the three measures: 3% normal conditions, 2% with medical device) showing a systematic reduction with the prosthesis (30% on average). This study demonstrated that masseter strain analysis is a repeatable and sensitive tool for the study of functional analysis of the masticatory organ. This opens new technical perspectives for the diagnosis and therapy of dysfunctional pathologies of the masticatory organ.

The masseter is a superficial muscle, which can be easily accessed by ultrasound equipment using high frequency, linear and real time probes. High frequency provides a detailed representation of the structures under examination and linear sensors are easily adaptable to the surfaces of the cheek while avoiding image distortions. In this way, masseter ultrasound permits a structural evaluation of the muscle (thickness, epimysium, perimysium) whose regular comb-like structure is made up by three, well oriented, layers and results in a relatively complex echogenicity. These structural parameters correlate with the anatomic integrity of the muscle and its tropism.

Ultrasound imaging in Real Time also enables the visualization of the muscle during its movement. This allows recognizing anatomic alterations during stress phases that cannot be detected at rest. In addition, acquisition of time sequences could allow, in principle, the evaluation of physiological characteristics of the muscle during its movement and an assessment of its functional properties. Functional evaluation could be useful to integrate the structural, anatomical information because the masseter is expected to be able to control the deformation in the different regions for changing the mechanical gain of the human mandibular lever (1).

The masseter muscle represents an area of

Key words: masseter muscle, strain imaging, skeletal muscle ultrasound

Mailing address:
Gianni Pedrizzetti,
Dept. Engineering and Architecture,
University of Trieste,
P.le Europa 1, 34127 Trieste, Italy
Tel.: +39 348 222 3223
e-mail: giannip@dica.units.it

0393-974X (2015)
Copyright © by BIOLIFE, s.a.s.
This publication and/or article is for individual use only and may not be further reproduced without written permission from the copyright holder.
Unauthorized reproduction may result in financial and other penalties
DISCLOSURE: ALL AUTHORS REPORT NO CONFLICTS OF INTEREST RELEVANT TO THIS ARTICLE.

important echo-functional interest for its relevance to mastication. It also permits other useful functions such as chewing, swallowing or speaking, and is involved in activities with no specific purpose such as clenching or grinding teeth. Movements are made possible by the temporomandibular joints which are carried out by mean of the forces generated by the muscles. Teeth, by virtue of their number, volume, shape, orientation and position, primarily influence the magnitude and direction of these forces. As a result, teeth and muscles work synergistically to provide an efficient and ecologic function. The mandibular joint is also designed to work with a right-left symmetry. The comparative evaluation of the activity of the right and left masseters could allow to identify whether the mandibular function develops in a symmetric pattern. The loss of the functional symmetry of the masticatory musculature is sometime associated with the development of numerous pain syndromes of the musculoskeletal system(2).

The muscular activity can be visualized by following the motion of the tissue imaged on ultrasound recordings. Tissue tracking techniques are known as two-dimensional (2D) optical flow (3, 4) and have been used in many research fields. They are commonly referred to as "speckle tracking" in echographic (B-mode) imaging when such displacements are used to follow physiological motion (5). Moreover, once the tissue elements are followed during their motion, it is possible to assess the deformation or strain of individual regions. Strain analysis can be physiologically significant for a muscle as it directly reflects the muscular activity in terms of contraction or stretching. Strain analysis in speckle tracking echocardiography was successfully introduced about one decade ago (6-8) and is now a largely diffused approach to the quantification of the contractile function of the myocardium (9). Application to skeletal muscles was introduced more recently (10-14), however its application to the masseter has not yet been verified. Electromyography was previously applied to masseter to describe the electrical phenomena that occur during muscle contraction, however, it does not provide a direct biomechanical analysis of the masticatory organ during its function.

The present research aims to verify the technical feasibility of speckle tracking echography in the masseter muscle for quantifying its muscular deformation pattern. Images are acquired during active closure to evaluate musculature function during its basic para-functional activity. In particular, this study aimed to provide evidence of the following aspects: (i) repeatability of the evaluation process, by verifying whether comparable results in terms of strain patters are obtained when the conditions of the experiment are replicated during a second procedure; (ii) sensitivity of the quantification process, by verifying the ability of muscular strain properties to differentiate between small induced variations to the masticatory organ. The objective is that of providing a ground support for translating this method toward clinical application.

MATERIALS AND METHODS

Clinical and ultrasound procedure

We enrolled 15 consecutive heterogeneous subjects who were directed to our studio during a complete physiatric check-up. None of them presented evidence of clinically relevant pathologies with the exception of occasional back pain of different entity - from slight to strong - which was present in most of them. All participants gave their written informed consent to participate in this study, which was carried out according to the declaration of Helsinki and was approved by the Institution's Ethics Committee.

All participants preliminarily underwent the normal orthodontic examination procedure to assess the mechanical structural and functional analysis of the masticatory organ. Afterward, they underwent an ultrasound examination of the masseter muscle in its superficial, intermediate and deep portions. Before the examination, it was necessary to identify the cutaneous projection of the masseter muscle, mark the identified area and isolate the area in a way to allow the repeatable positioning of the ultrasound probe. To this purpose, a lateral view photograph was taken and the landmarks were identified and connected therein with straight lines as shown in Fig. 1a. The same landmarks were then identified on the patient and, using the photograph as reference, the same connecting lines were drawn on the skin with a non-permanent cutaneous marker as shown in Fig. 1b. The ultrasound recordings were performed with the subject seated in the dental chair. The mechanical holder arm shown in Fig. 1c was used to immobilize the ultrasound probe at the specified position.

Echography was performed with Esaote MyLabOne

equipped with a wideband (13- 6MHz) electronic linear probe SL3323 (Esaote SpA, Genoa, Italy) with a 40-mm footprint. Images were taken starting from rest, during active teeth clenching for about 3 seconds using a bar of balsa with standard size until it is crushed, and ending at rest. The duration of the entire recording rest-clenching-rest varied from 7 to 10 seconds acquired with a sample frequency about 20 Hz.

The ultrasound examination was performed under natural conditions and, immediately afterwards, after the positioning of a temporary medical device (partial resin prosthesis Jig). This device altered the distance between the dental arches by 2 mm and was designed to modify muscular recruitment during the occlusion of the mouth. This is a standard device, shown in Fig. 1d, employed in medical practice to verify and eliminate nighttime clenching (bruxism) by altering the mechanical gain of the mandibular lever.

The entire procedure (preparation + recordings without and with device) was repeated three times, on a second day and a third day. For a total of six recordings per participant. Ultrasound image sequences were then evaluated by a prototype software (Muscle Dynamics Ver. 1.6.2.0, AMID SRL, Sulmona, AQ, Italy), which computes the strain values at every point during the recording period, as described below. The software permits to visualize the strain pattern inside a previously defined region of interest and to draw the strain curves at every point or area therein. Fig. 2 shows an example of the ultrasound image at rest recorded by the echograph (Fig. 2a), with a grid superimposed on the image (Fig. 2b) and its deformation during contraction (Fig. 2c).

The comparison between images of the deformation fields corresponding to different recordings were primarily carried out by visual assessment. A quantitative comparison was then provided by reporting the value of peak deformation in the deep portion of the masseter during maximal contraction. There, the strain distribution was relatively uniform and its value, given the repetitive protocol, provided an initial indication about changes in deformation pattern.

STRAIN COMPUTATION

Tissue tracking

The first step for the evaluation of the muscle deformation required the identification of the tissue motion from the B-mode sequence of images. To this aim, a region of interest was manually drawn on the image in the frame corresponding to the initial, undeformed rest state. Here a regular grid was automatically drawn, with 16 pixels spacing, and the individual grid points were tracked in time from one frame to the next.

The automatic evaluation of the tissue displacement at every point is determined from comparing the gray-scale image data about such point in two consecutive frames using an optical flow approach. Such methods are largely present in literature, the details of the present application are reported below. Following previous studies in echocardiography (6, 8) as well as in skeletal muscle ultrasound (12), tracking is performed by estimating the displacements (δ_x, δ_y) along the two Cartesian directions respectively, that minimize the square error E

$$E = \sum \left(\frac{\partial B}{\partial t} + \delta_x \frac{\partial B}{\partial x} + \delta_y \frac{\partial B}{\partial y} \right)^2 ; \text{ (i)}$$

of the advection equation for the brightness B of the ultrasound image. Time derivative indicates the difference between two consecutive frames and the spatial derivatives are averaged between the same frames. The summation in (i) is computed over a square window centered at the interrogating points and the minimization of (i) leads to a linear system where the unknown are the frame-by-frame displacements δ_x, δ_y. The analysis is performed in three steps using a so-called coarse-to- fine approach, reducing the window size from 32x32 to 16x16 to 8x8; the position of the interrogation point is continuously updated with the displacements integrated on the previous frames to end up with the tracking of the tissue points. Previously applications to echocardiography for tracking the myocardial muscle found that a frame rate of acquisition higher than 60 Hz (about >50 frames per heartbeat) was suggested (15). To comply with this requirement, we employed here over 140 frames during a single deformation cycle.

The moving tissue, obtained from 2D tissue tracking, is eventually described by the coordinates of its moving points $\mathbf{X}(s_1,s_2,t)$, being the vector $\mathbf{X}=[X,Y]$. The parametric coordinates s_1 and s_2 coincide with Cartesian coordinates at the undeformed (initial) condition and then identify the material points following the tissue motion during the deformation (Lagrangian, or material, coordinates). The 2D velocity vector of the tissue is defined at every point as the time derivative of the position vector $\mathbf{V}(s_1,s_2,t)=d\mathbf{X}/dt$.

Evaluation of strain

Strain-rate represents an instantaneous physical property and, as such, it is well suited for describing deformation rate on a moving reference because it depends on the instantaneous properties of the reference systems and not on the previous history. The strain-rate tensor $\mathbf{SR}(s_1,s_2,t)$ is defined by the symmetric part of the gradient of velocity (16)

$$\mathbf{SR}(s_1, s_2, t) = \begin{bmatrix} \frac{1}{h_1}\frac{\partial \mathbf{V}}{\partial s_1} \bullet \boldsymbol{\tau}_1 & \frac{1}{2}\left(\frac{1}{h_1}\frac{\partial \mathbf{V}}{\partial s_1} \cdot \boldsymbol{\tau}_2 + \frac{1}{h_2}\frac{\partial \mathbf{V}}{\partial s_2} \cdot \boldsymbol{\tau}_1\right) \\ \frac{1}{2}\left(\frac{1}{h_1}\frac{\partial \mathbf{V}}{\partial s_1} \cdot \boldsymbol{\tau}_2 + \frac{1}{h_2}\frac{\partial \mathbf{V}}{\partial s_2} \cdot \boldsymbol{\tau}_1\right) & \frac{1}{h_2}\frac{\partial \mathbf{V}}{\partial s_2} \bullet \boldsymbol{\tau}_2 \end{bmatrix}, \text{(ii)}$$

whose off-diagonals elements are pair-wise equal. In (ii) the coordinate metrics $h_1(s_1,s_2,t)$ and $h_2(s_1,s_2,t)$, given by $h_1^2=(dX/ds_1)^2+(dY/ds_1)^2$ and $h_2^2=(dX/ds_2)^2+(dY/ds_2)^2$ represent the unit length along the coordinate lines. Moreover, the directional units vectors, $\mathbf{t}_1(s_1,s_2,t)=h_1^{-1}d\mathbf{X}/ds_1$ and $\mathbf{t}_2(s_1,s_2,t)=h_2^{-1}d\mathbf{X}/ds_2$, directed toward the increasing direction of the corresponding coordinate, are employed to comply with the non-Cartesian reference system in the generic deformed tissue configuration (9).

The natural definition of the 2D Strain tensor $\mathbf{St}(s_1,s_2,t)$ is then obtained by time-integration of the strain-rate

$$\mathbf{St}(s_1, s_2, t) = \int_0^t \mathbf{SR}(s_1, s_2, t)dt = \begin{bmatrix} St_1 & Sh \\ Sh & St_2 \end{bmatrix}; \text{(iii)}$$

where integration is initiated at the undeformed instant (here generically indicated with $t=0$).

Strain (iii) is a symmetry tensor by construction. This ensures the existence of a special system of coordinates such that, relative to them, the same strain tensor can be described by two strain values (eigenvalues) along those coordinates and zero shear. The eigenvalues of the strain tensor (iii) are called principal strain, and they act along the principal directions which are the corresponding eigenvectors. Principal strain values are ordered from the smallest (most negative) to the largest to describe the compression and dilatation straining in the tissue, $St_C(s_1,s_2,t)$ and $St_D(s_1,s_2,t)$, respectively. They are computed by the components in equation (iii)

$$St_C(s_1, s_2, t) = \frac{1}{2}\left(St_1 + St_2 - \sqrt{(St_1 + St_2)^2 + 4Sh^2}\right),$$
$$St_D(s_1, s_2, t) = \frac{1}{2}\left(St_1 + St_2 + \sqrt{(St_1 + St_2)^2 + 4Sh^2}\right); \text{(iv)}$$

and the principal direction makes an angle $\tan^{-1}(Sh/(St_1-St_2))$ with the original coordinates s_1,s_2.

These strain values represent the entity of deformation on the image plane only. However, the image represents only a slice of the 3D tissue that also deforms in the cross-plane direction, under the assumption that mass is conserved, it is possible to estimate the value of cross-plane strain as $St_X(s_1,s_2,t)=-St_C-St_D$. The so-computed cross-plane strain also corresponds to the local reduction or increase of the area in the image and is therefore a comprehensive measure, in 2D imaging, of local contraction and dilatation.

RESULTS

The patterns of deformation repeated themselves with uniformity when the conditions of the experiment were not varied; consistently, the patterns changed when conditions were varied.

The three rows of Fig. 3 show the cross-plane strain patterns in the masseter muscle for one patient (patient # 12) under the condition of maximum clenching of the teeth recorded in three different days. The three images on the first column (Fig. 3 a-c) show the normal behavior without any medical device; the three images on the second column (Fig. 3 d-f) show the same results after the positioning of the temporary medical device, which should alter the occlusion. These example images give evidence that the strain pattern is highly comparable between different recordings performed under the same conditions either normal or with medical device. They also support evidence of the alteration of the strain pattern when the patient carried out clenching of the teeth after introducing a measured medical device in the mouth.

The same behavior was found on the entire population analyzed. The repeatability under the same conditions and the modification under altered conditions are confirmed by inspection of the same six-images recorded on every individual patient.

Numerical results of all the participants are reported in Table I. They show comparable strain value for the different recordings in natural contractions (average values: day 1, 44.7%; day 2, 44.6%; day 3, 44.9%) that differ from those in presence of the prosthesis (average values: day 1, 14.5%; day 2, 13.7%; day 3, 16.7%). The intra-individual variability is quantified by the standard deviation computed from the 3 measurements (average values: natural contraction 3.16%; with prosthesis 2.19%); the paired Student-*t* test between the 3 pairs in the two conditions is not significant ($p>0.1$). The paired Student-*t* test between measurements performed on the same day with and without the device show significant differences ($p<0.0001$).

The visual inspection of the strain pattern also demonstrated that the natural muscular deformation develops synergistically over the different masseter regions. The presence of the prosthesis reduced the ability to contract in the deep posterior region of the

Table I. *Peak values of the cross-strain evaluated during maximum contraction in the deep portion of the masseter muscle.*

Participant #	Natural contraction				With Prosthesis				
	Day 1	Day 2	Day 3	STD	Day 1	Day 2	Day 3	STD	DIFF
1	32%	30%	34%	1.6%	0%	2%	0%	0.9%	-31%
2	37%	30%	33%	2.9%	0%	0%	0%	0.0%	-33%
3	55%	58%	50%	3.3%	35%	30%	29%	2.6%	-23%
4	89%	83%	81%	3.4%	32%	34%	30%	1.6%	-52%
5	45%	48%	50%	2.1%	26%	20%	29%	3.7%	-23%
6	18%	15%	16%	1.3%	39%	40%	45%	2.6%	25%
7	55%	58%	62%	2.9%	34%	30%	36%	2.5%	-25%
8	34%	36%	30%	2.5%	20%	14%	26%	4.9%	-13%
9	68%	70%	75%	2.9%	0%	0%	2%	0.9%	-70%
10	59%	50%	55%	3.7%	0%	0%	3%	1.4%	-54%
11	44%	40%	36%	3.3%	20%	24%	19%	2.2%	-19%
12	40%	43%	38%	2.1%	0%	0%	0%	0.0%	-40%
13	26%	39%	40%	6.4%	2%	2%	18%	7.5%	-28%
14	36%	37%	30%	3.1%	6%	6%	9%	1.4%	-27%
15	32%	30%	44%	6.2%	3%	3%	4%	0.5%	-32%
Average	**45%**	**44%**	**45%**	**3.2%**	**14%**	**14%**	**17%**	**2.2%**	**-30%**

The intra-individual variability (STD) is computed by the standard deviation within the three different acquisitions. The strain difference (DIFF) after prosthesis insertion is reported in the last column.

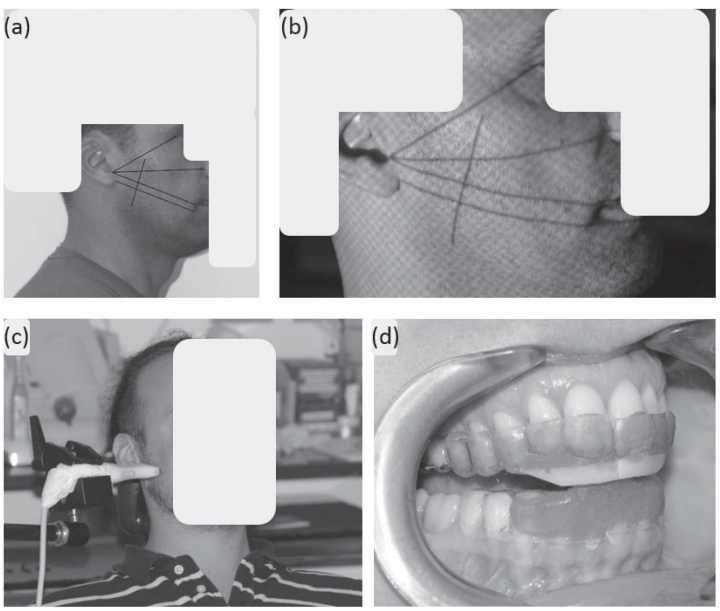

Fig. 1. *Preparation of the ultrasound exam. Anatomical landmarks are first drawn on a side view photograph (**a**), then they are projected and marked on the patient's skin (**b**). The ultrasound probe shown in the picture is positioned by a mechanical arm with the patient sitting in a dental chair (**c**). The medical device modifies teeth clenching by altering the mechanical gain of the mandibular lever (**d**).*

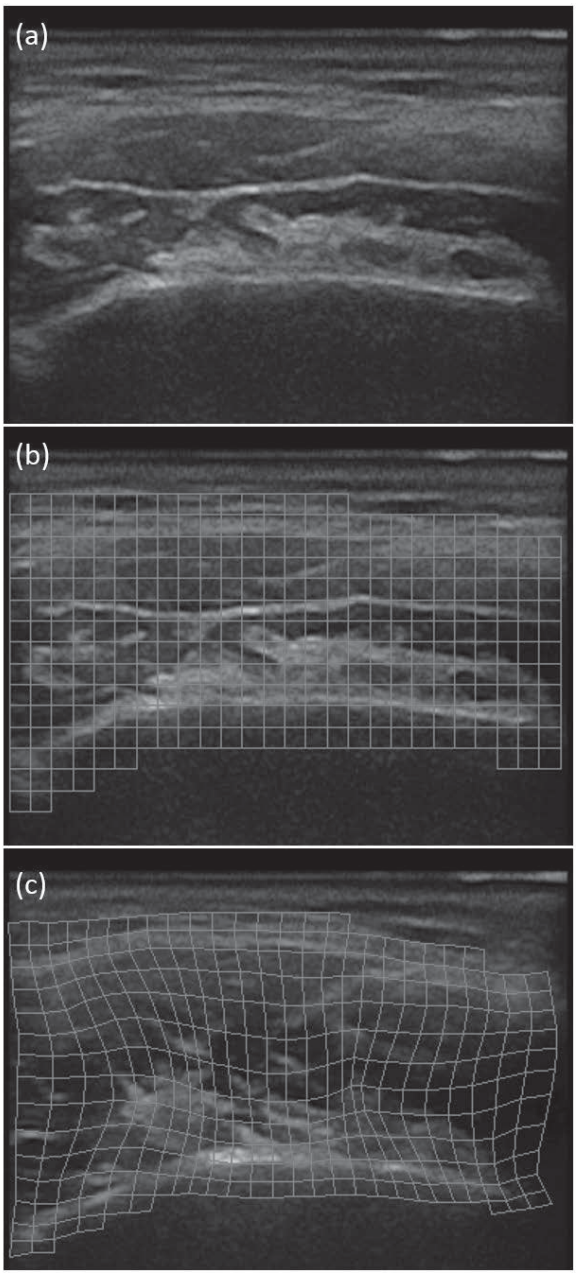

Fig. 2. *Ultrasound image of the masseter muscle at rest recorded by the echograph (**a**). The same image with a virtual grid superimposed on the masseter area (**b**). The ultrasound image during teeth clenching with the superimposed deformed grid computed by the present method (**c**).*

masseter muscle in all participants with a reduction ranging from 13% to 70% (average 30%) (Table I). A comparable reduction in the superficial anterior region is found in a much smaller percentage of participants.

DISCUSSION

Muscular strain analysis has a long history for applications in cardiology, nevertheless its applications to musculature is still limited. This study demonstrated, for the first time, the technical feasibility of the muscular strain analysis applied to the masseter muscle.

It was demonstrated that the masseter could be studied in terms of deformation during muscle contraction by means of ultrasound combined with the application of strain analysis. The technique presented a high repeatability during multiple acquisitions when the conditions of the acquisition were not varied. The technique appeared also capable of detecting variations of the masseter muscle during contraction after variations of the clinical conditions. This suggests that ultrasound could be a sensitive tool to evaluate conditions of physiological interest, although its clinical relevance will have to be confirmed in systematic studies.

These first results show, for the first time, that the deformation of the masseter muscle during contraction is not spatially uniform or gradually varied. The deformation develops along specific deformation patterns which are modified in different conditions. The quantitative comparison was performed for the deep portion of the muscle, where the strain distribution is relatively uniform. The deformation value therein represents an initial indicator of differences in the contraction pattern, demonstrating that the prosthesis provokes a systematic reduction of deep muscle strain in all participants. The deep portion is also considered of particular interest when exploring the potential influence between stresses in the masseter and those in the muscles of the back kinetic chain.

The analysis presented here is aimed to verify the feasibility of the ultrasound approach. The positive results suggest that this technique can be implemented for the study of the functional behavior of mastication musculature, such as mastication, swallowing, and phonation, as well as para-functional activities, such as grinding and clenching of teeth. This preliminary evidence opens new perspectives for a more in depth

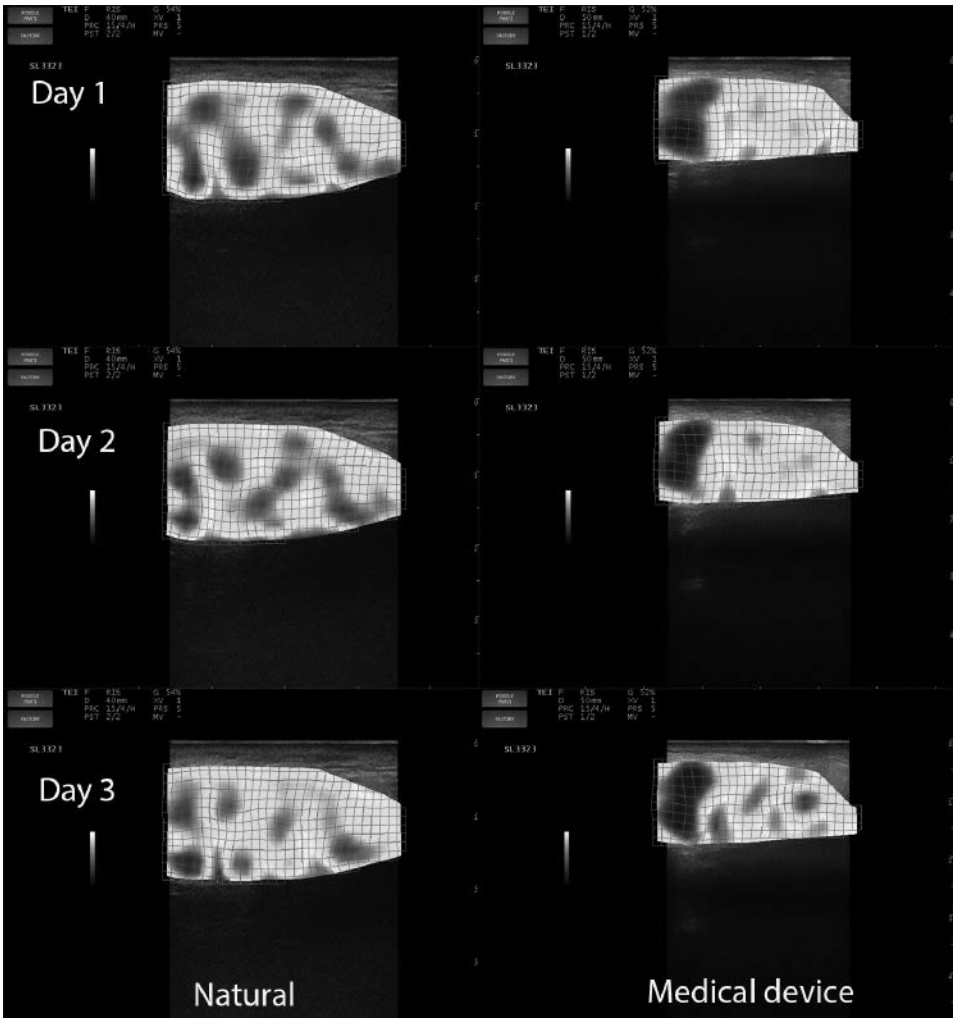

Fig. 3. *Strain pattern of the masseter muscle at the maximal contraction during teeth clenching reported over the original ultrasound image. Cross-plane strain pattern is reported with colors from blue to red (blue means negative cross-plane strain, thus areal expansion of the image plane; red is positive cross-plane strain, thus areal contraction of the plane). The three images on the first column (**a-c**) correspond to the natural condition; the three-images on the second column (**d-e**) are recorded after the insertion of a medical device that alters teeth occlusion. The three rows correspond to the images acquired on three different days.*

investigation of either the diagnosis or the therapy of several dysfunctional pathologies of the human mandibular function.

This study analyses the deformation in the 2D image plane only. This represents a partial perspective of the effective muscular deformation that is three-dimensional. A more comprehensive evaluation of the muscular activity could be performed using several probe locations to measure the strain in the other planes (17) or by using three-dimensional ultrasound acquisitions.

The deformation of the masseter muscle can be evaluated by ultrasound, which demonstrated to be a reliable, repeatable and sensitive technique for moving into clinical studies of functional analysis of the masticatory organ dealing with dysfunctional pathologies.

REFERENCES

1. Hylander WL, Ravosa MJ, Ross CF, Wall CE, Johnson KR. Symphyseal fusion and jaw-adductor

muscle force: an EMG study. Am J Phys Anthropol 2000; 112(4):469-492.
2. Rocha CP, Croci CS, Caria PH. Is there relationship between temporomandibular disorders and head and cervical posture? A systematic review. J Oral Rehabil 2013; 40(11):875-881.
3. A. S. Optic Flow Computation: A Unified Perspective. Piscataway, NJ: IEEE Comput. Soc. 1992.
4. Barron JL, Fleet DJ, S. B. Performance of optical flow techniques. International Journal of Computer Vision 1994; 12:43-77.
5. Bohs LN, Geiman BJ, Anderson ME, Gebhart SC, Trahey GE. Speckle tracking for multi-dimensional flow estimation. Ultrasonics 2000; 38(1-8):369-375.
6. Malpica N, Santos A, Zuluaga MA, Ledesma MJ, Perez E, Garcia-Fernandez MA, Desco M. Tracking of regions-of-interest in myocardial contrast echocardiography. Ultrasound Med Biol 2004; 30(3):303-309.
7. Leitman M, Lysyansky P, Sidenko S, Shir V, Peleg E, Binenbaum M, Kaluski E, Krakover R, Vered Z. Two-dimensional strain-a novel software for real-time quantitative echocardiographic assessment of myocardial function. J Am Soc Echocardiogr 2004; 17(10):1021-1029.
8. Vannan MA, Pedrizzetti G, Li P, Gurudevan S, Houle H, Main J, Jackson J, Nanda NC. Effect of cardiac resynchronization therapy on longitudinal and circumferential left ventricular mechanics by velocity vector imaging: description and initial clinical application of a novel method using high-frame rate B-mode echocardiographic images. Echocardiography 2005; 22(10):826-830.
9. Pedrizzetti G, Sengupta S, Caracciolo G, Park CS, Amaki M, Goliasch G, Narula J, Sengupta PP. Three-dimensional principal strain analysis for characterizing subclinical changes in left ventricular function. J Am Soc Echocardiogr 2014; 27(10):1041-1050 e1041.
10. Loram ID, Maganaris CN, Lakie M. Use of ultrasound to make noninvasive in vivo measurement of continuous changes in human muscle contractile length. J Appl Physiol (1985) 2006; 100(4):1311-1323.
11. Yoshii Y, Villarraga HR, Henderson J, Zhao C, An KN, Amadio PC. Speckle tracking ultrasound for assessment of the relative motion of flexor tendon and subsynovial connective tissue in the human carpal tunnel. Ultrasound Med Biol 2009; 35(12):1973-1981.
12. Peolsson M, Lofstedt T, Vogt S, Stenlund H, Arndt A, Trygg J. Modelling human musculoskeletal functional movements using ultrasound imaging. BMC Med Imaging 2010; 10:9.
13. Korstanje JW, Schreuders TR, van der Sijde J, Hovius SE, Bosch JG, Selles RW. Ultrasonographic assessment of long finger tendon excursion in zone v during passive and active tendon gliding exercises. J Hand Surg Am 2010; 35(4):559-565.
14. Darby J, Hodson-Tole EF, Costen N, Loram ID. Automated regional analysis of B-mode ultrasound images of skeletal muscle movement. J Appl Physiol (1985) 2012; 112(2):313-327.
15. Mor-Avi V, Lang RM, Badano LP, et al. Current and evolving echocardiographic techniques for the quantitative evaluation of cardiac mechanics: ASE/EAE consensus statement on methodology and indications endorsed by the Japanese Society of Echocardiography. Eur J Echocardiogr 2011; 12(3):167-205.
16. Pedrizzetti G, Kraigher-Krainer E, De Luca A, et al. Functional strain-line pattern in the human left ventricle. Phys Rev Lett 2012; 109(4):048103.
17. Lopata RG, van Dijk JP, Pillen S, et al. Dynamic imaging of skeletal muscle contraction in three orthogonal directions. J Appl Physiol (1985) 2010; 109(3):906-915.